

## Supplementary Information

### Hierarchically core-shell Ni@C-NCNTs nanocomposites tailored for microwave-induced dry reforming of methane process

Miaomiao Zhang<sup>a</sup>, Yibo Gao<sup>a</sup>, Yanpeng Mao<sup>a,\*</sup>, Yang Jin,<sup>a</sup> Wenlong Wang<sup>a</sup>, Jian Sun<sup>b</sup>, Zhanlong Song<sup>a</sup>, Jing Sun<sup>a</sup>, Xiqiang Zhao<sup>a</sup>

- a. *National Engineering Laboratory for Reducing Emissions from Coal Combustion, Engineering Research Center of Environmental Thermal Technology of Ministry of Education, Shandong Key Laboratory of Energy Carbon Reduction and Resource Utilization, School of Energy and Power Engineering, Shandong University, Jinan, Shandong, 250061, China*
- b. *Dalian National Laboratory for Clean Energy, Dalian Institute of Chemical Physics, Chinese Academy of Sciences, 116023, Dalian, China*

\*Corresponding author. Phone +86 531 88399372, Fax +86 531 88395877. E-mail:  
[maoyanpeng@sdu.edu.cn](mailto:maoyanpeng@sdu.edu.cn)

## **1. Catalysts characterization**

The X-ray diffraction (XRD) analysis of the catalysts was carried out on a Bruker D8 Advance diffractometer with Cu K $\alpha$  radiation and an operating voltage of 40 kV and current of 40 mA.

The concentrations of metal ions in the test samples were determined by an inductively coupled plasma-optical emission spectrometer (ICP-OES, Perkin Elmer optima-7000DV). Based on the standard method HJ 832–2017 (CN), MSWI-FA was digested by the optimized HNO<sub>3</sub>-HCl method using a microwave digester (SINEO, MDS-6C).

N<sub>2</sub>-adsorption was carried out at -196 °C using Quantachrome Instruments Autosorb-iQ and the specific surface areas and the pore size distributions of the samples were determined based on the Brunauer–Emmett–Teller (BET) model and the Barrett–Joyner–Halenda (BJH) method, respectively.

The morphologies, structures and related elemental mapping information were obtained via scanning electron microscopy (SEM, Carl Zeiss AG/SUPRA55TM) and transmission electron microscopy (TEM, ThermoFischer Talos F2000x), respectively.

X-ray photoelectron spectroscopy (XPS) analysis was performed in a ThermoFisher Scientific spectrometer using an Al K $\alpha$  X-ray source (energy = 1486.6 eV).

H<sub>2</sub> temperature-programmed reduction (H<sub>2</sub>-TPR) to evaluate the reducibility of the prepared catalysts on Quantachrome ChemBet Pulsar apparatus, equipped with thermal conductivity detector (TCD). About 50 mg of samples were loaded and 3% H<sub>2</sub>/He was used as reductant (He for pretreating at 200 °C for 0.5 h followed by cooling to room temperature, H<sub>2</sub>/He mixture for heating up to 800 °C at a heating rate of 10 °C/min).

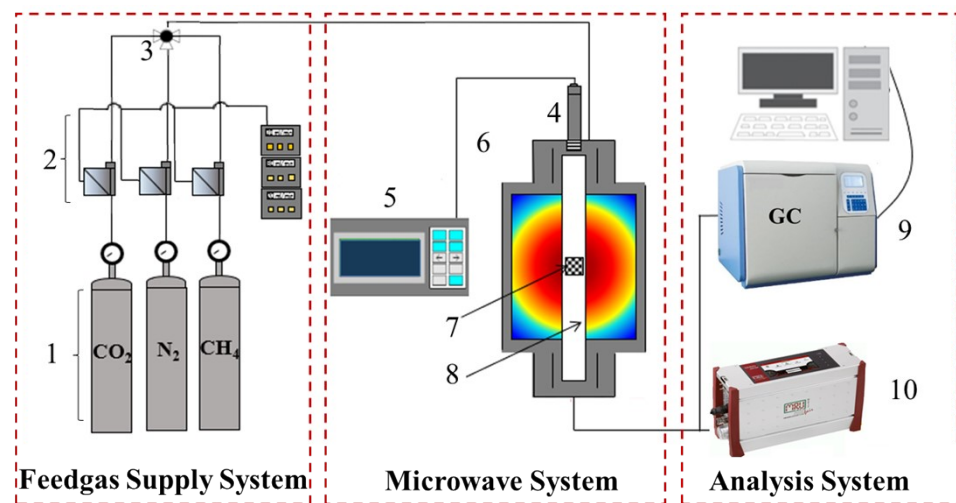
The magnetic hysteresis loops were made using a LakeShore 7404 (LakeShore, USA) vibrating sample magnetometer (VSM).

Raman spectra of powder samples were recorded using a laser confocal Raman spectrometer (XploRA, Horiba Jobin Yvon, Ltd.) with laser excitation wavelength of 532 nm.

The Thermogravimetric analysis (TGA) of the samples was performed with a thermogravimetric analyzer (Mettler Toledo), which was used to explore the carbon content and formation of the samples. In the TGA experiment, the samples were heated from 25 to 900 °C at a constant heating rate of 10 °C/min under an air flow of 50 mL/min.

The electromagnetic parameters of all the samples were measured at 2–18 GHz on a vector network analyzer (VNA, E5071C, Agilent, USA) via the coaxial-line method. The samples were prepared by uniformly mixing the composites (30 wt%) and paraffin (70 wt%) at 80 °C and pressed into toroidal rings with an outer diameter of 7 mm, an inner diameter of 3 mm, and a thickness of 3 mm.

## 2. Supporting Figures



1. gas cylinder; 2. flow meter; 3. gas mixing tank; 4. infrared thermometer; 5. microwave power source
6. microwave reaction chamber; 7. sample; 8. quartz tube; 9. gas chromatography; 10. flue gas analyzer

**Scheme S1. Schematic configuration for the microwave catalytic reaction system.**

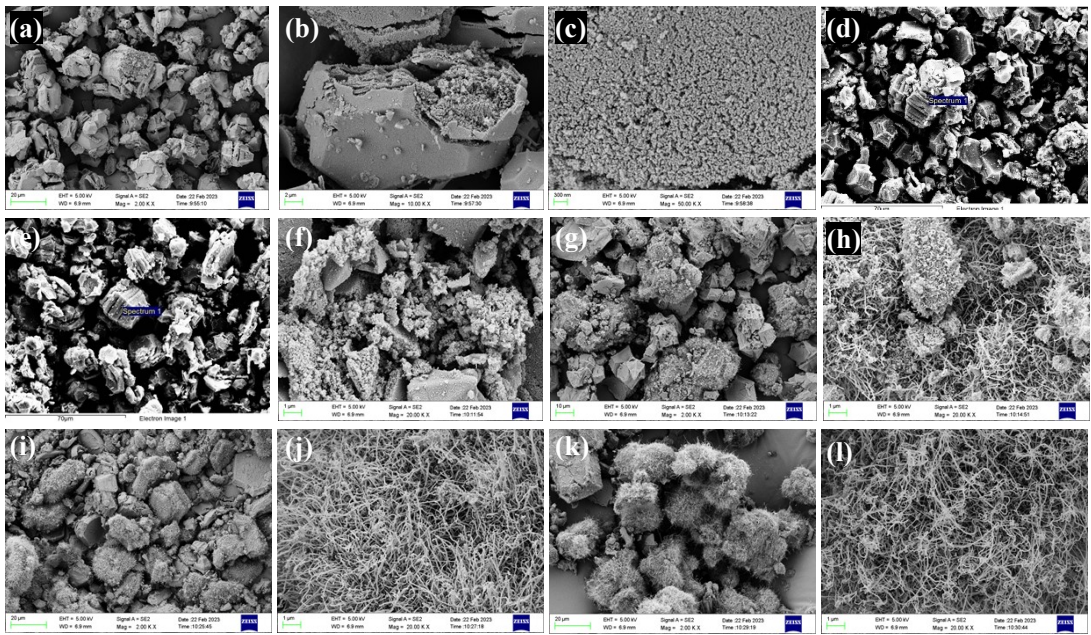


**Fig.S1. SEM images for (a-c) Ni@C-500, (d) Ni@C-800, (e-f) Ni@C-NCNTs-2, (g-h) Ni@C-NCNTs-5, (i-j) Ni@C-NCNTs-8, (k-l) Ni@C-NCNTs-10.**

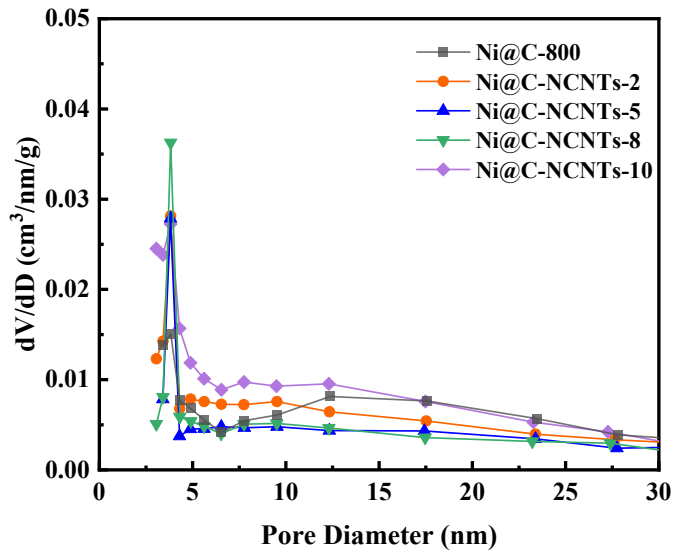


**Fig.S2. Pore size distribution.**

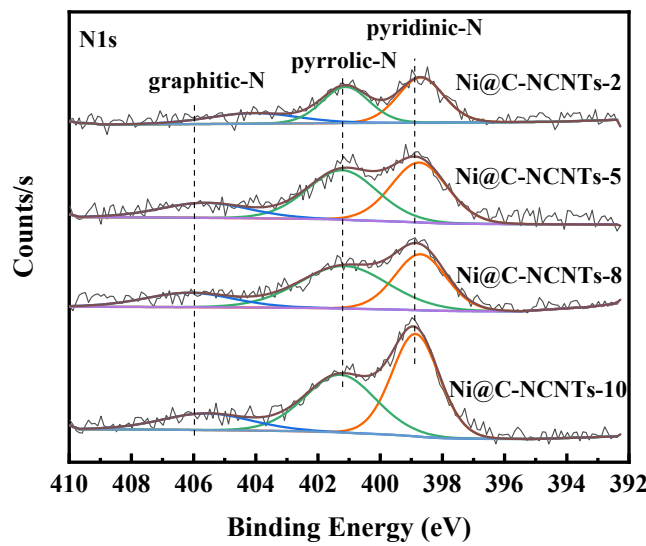


**Fig.S3. XPS spectra of the samples.**

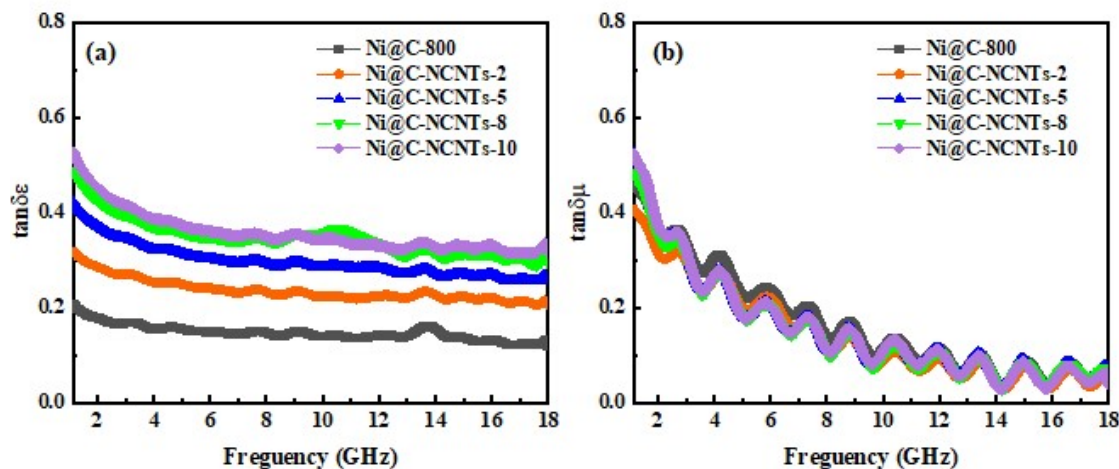


**Fig.S4. Electromagnetic parameters of Ni@C-800 and the N@C @NCNTs composites: (a) dielectric loss  $\tan\delta\epsilon$  and (b) magnetic loss  $\tan\delta\mu$ .**

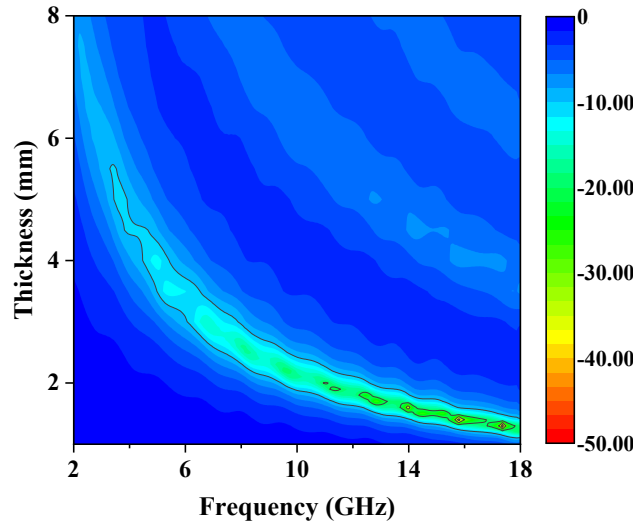


**Fig.S5. Three-dimensional reflection loss plot of Ni@C-NCNTs-10.**

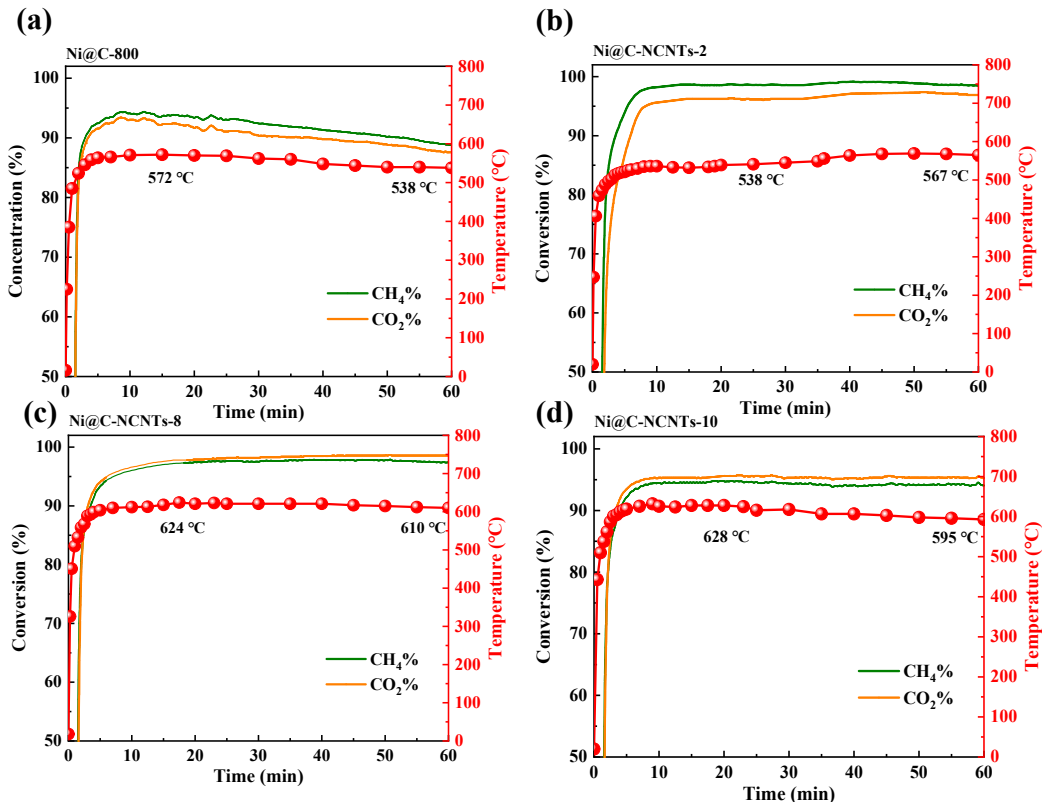


**Fig.S6. Catalytic process with in-situ measured top surface temperature by the IR pyrometer for (a) Ni@C-800 (b) Ni@C-NCNTs-2, (c) Ni@C-NCNTs-8, (d) Ni@C-NCNTs-10 in the MW-DRM process at 80 W. (Reaction conditions: catalyst dosage = 1 g, CH<sub>4</sub>: CO<sub>2</sub>: N<sub>2</sub> = 15: 15: 70, gas hourly space velocity = 9600 mL/g·h).**

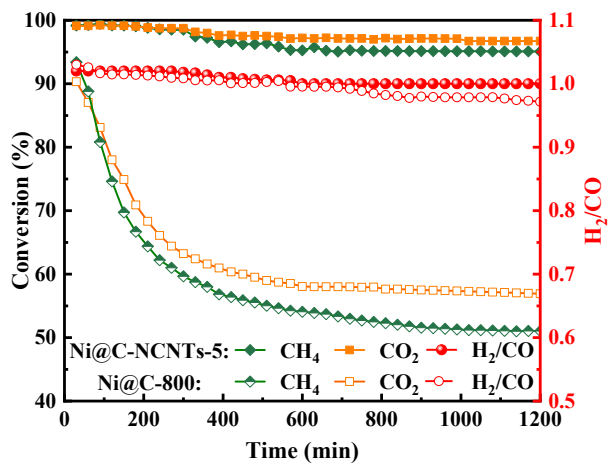


**Fig. S7. MW-DRM stability experiment of Ni@C-800 and Ni@C-NCNTs-5 for 20 h. (Experimental conditions: catalyst dosage = 1 g, MW power = 100W, gas hourly space velocity = 9600 mL/g·h, CH<sub>4</sub>:CO<sub>2</sub> = 1:1)**

### 3. Supporting Tables

**Table S1. Elemental mapping results for the catalysts (wt.%).**

Sample	Ni@C-800	Ni@C-NCNTs-2	Ni@C-NCNTs-5	Ni@C-NCNTs-8	Ni@C-NCNTs-10
C	15.21	22.39	46.37	47.24	48.74
N	-	6.70	13.57	13.73	14.28
O	1.27	3.09	4.03	4.13	4.31
Ni	83.52	67.83	36.03	34.90	32.67
Totals	100.00	100.00	100.00	100.00	100.00

**Table S2 Surface nickel and nitrogen contents (%) of different catalysts determined by XPS**

Catalysts	Relative content of Ni species		Relative content of N species		
	Ni <sup>2+</sup>	Ni <sup>0</sup>	graphitic-N	pyrrolic-N	pyridinic-N
Ni@C-800	54.45	45.55	--	--	--
Ni@C-NCNTs-2	70.06	29.94	16.71	40.88	42.41
Ni@C-NCNTs-5	69.60	30.40	15.02	42.09	42.89
Ni@C-NCNTs-8	82.64	17.36	14.15	42.31	43.54
Ni@C-NCNTs-10	100.00	--	14.00	40.07	45.93

**Table S3. The surface and bulk temperature of the catalyst bed for the Ni@C-NCNTs-5 at equilibrium during MW-DRM.**

MW Power ( W )	Surface temperature, T <sub>sur</sub> (°C)	Bulk temperature T <sub>bulk</sub> (°C)	CH <sub>4</sub> Conversion (%)	CO <sub>2</sub> Conversion (%)
40	437	625	53.33	48.84
60	536	738	95.3	93
80	628	820	99.3	98.7
100	677	879	99.99	99.6
120	706	904	100	99.99

**Table S4. Comparison of catalytic performance of different studies on microwave-induced methane dry reforming**

Catalysts	Dosage (g)	Experimental conditions			CH <sub>4</sub> conversion (%)	CO <sub>2</sub> conversion (%)	H <sub>2</sub> /CO ratio
		GHSV (mL/g·h)	MW (W)	T (°C)			
Ni@C-NCNTs-5 (This work)	1.0	9600	100	620	99.3	98.7	1.02
Activated carbon <sup>1</sup>	8.0	320	800	800	75-100	79-100	0.8
Ni-La <sub>2</sub> O <sub>3</sub> /AC <sup>2</sup>	1.0	9600	100	600	96.2	99.1	0.98
Ni/Al <sub>2</sub> O <sub>3</sub> +AC <sup>3</sup>	6.0	1500	142	800	88.1	93.3	--
Ni/Al <sub>2</sub> O <sub>3</sub> +bio-char <sup>4</sup>	6.0	1200	N.M. <sup>a</sup>	800	84-91	88-94	0.8
bio-char <sup>5</sup>	6.0	1200	450	975	~80	~90	0.88
Bio-char+Fe <sub>2</sub> O <sub>3</sub> <sup>6</sup>	3.0	2400	N.M. <sup>a</sup>	800	95	98	1.01

Ni/MgO/AC <sup>7</sup>	0.9	6700	N.M. <sup>a</sup>	650	~89	~90	~0.9
Ru/SrTiO <sub>3</sub> <sup>8</sup>	1.0	3000	150	702	93.9	~90	~0.9
Co–Mo/TiO <sub>2</sub> <sup>9</sup>	4.0	10000	100	--	81	86	~0.9
Co–Mo/Al <sub>2</sub> O <sub>3</sub> <sup>10</sup>	4.0	10000	200	--	80	93	0.8
Ni–Mn/ZrO <sub>2</sub> <sup>11</sup>	1.0	2000	100	180	94	93	~1.0
Cr -Ni/CeO <sub>2</sub> <sup>12</sup>	0.5	10200	500	850	90	92	1.45
Fe/SiC <sup>13</sup>	10	1200	900	750	93	92	0.98
Ni/SiC <sup>14</sup>	0.5	11000	60	800	96.3	88.7	0.85
Ni–Co/ZrO <sub>2</sub> –CaO <sup>15</sup>	1.0	7200	650	800	97.1	99.2	~1.0
Fe/HZSM-5/Biochar <sup>16</sup>	5.0	2400	700	850	63.03	91.27	0.9
Cr-LaNiO <sub>3–δ</sub> <sup>17</sup>	0.3	17000	600	961	~70	~85	--
La <sub>0.8</sub> Sr <sub>0.2</sub> Co <sub>0.9</sub> Mn <sub>0.1</sub> O <sub>3</sub> <sup>18</sup>	0.35	8570	90	850	83	90	0.93

a. N.M. means the value of applied MW power was not mentioned in the paper.

b. CH means conventional heating method was used as heat source in the experiment.

## Supplementary References

- 1 B. Fidalgo, A. Dominguez, J. Pis, J. Menendez, Microwave-assisted dry reforming of methane, *Int. J. Hydrogen Energ.*, 2008, 33, 4337-4344.
- 2 M. Zhang, Y. Gao, Y. Mao, W. Wang, J. Sun, Z. Song, J. Sun, X. Zhao, Enhanced dry reforming of methane by microwave-mediated confined catalysis over Ni-La/AC catalyst. *Chem. Eng. J.*, 2023, 451, 138616.
- 3 B. Fidalgo, J.A. Menéndez, Study of energy consumption in a laboratory pilot plant for the microwave-assisted CO<sub>2</sub> reforming of CH<sub>4</sub>, *Fuel Process. Technol.*, 2012, 95, 55-61.
- 4 L. Li, X. Jiang, H. Wang, J. Wang, Z. Song, X. Zhao, C. Ma, Methane dry and mixed reforming on the mixture of bio-char and nickel-based catalyst with microwave assistance, *J. Anal. Appl. Pyrol.*, 2017, 125, 318-327.
- 5 L. Li, J. Chen, K. Yan, X. Qin, T. Feng, J. Wang, F. Wang, Z. Song, Methane dry reforming with microwave heating over carbon-based catalyst obtained by agriculture residues pyrolysis, *J. CO<sub>2</sub> Util.*, 2018, 28, 41-49.
- 6 L. Li, K. Yan, J. Chen, T. Feng, F. Wang, J. Wang, Z. Song, C. Ma, Fe-rich biomass derived char for microwave-assisted methane reforming with carbon dioxide, *Sci. Total Environ.* 2019, 657, 1357-1367.
- 7 S. Sharifvaghefi, B. Shirani, M. Eic, Y. Zheng, Application of microwave in hydrogen production from methane dry reforming: Comparison between the conventional and Microwave-Assisted catalytic reforming on improving the energy efficiency, *Catalysts* ,2019, 127, 8940.
- 8 L.S. Gangurde, G.S.J. Sturm, M.J. Valero-Romero, R. Mallada, J. Santamaria, A.I. Stankiewicz, G.D. Stefanidis, Synthesis, characterization, and application of ruthenium-doped SrTiO<sub>3</sub> perovskite catalysts for microwave-assisted methane dry reforming, *Chem. Eng. Process*, 2018, 127, 178-190.

- 9 H.M. Nguyen, G.H. Pham, M. Tade, C. Phan, R. Vagnoni, S. Liu, Microwave-Assisted dry and bi-reforming of methane over m - Mo/TiO<sub>2</sub> (M = co, cu) bimetallic catalysts, *Energ. Fuel.*, 2020, 34, 7284-7294.
- 10 H.M. Nguyen, G.H. Pham, R. Ran, R. Vagnoni, V. Pareek, and S. Liu, Dry reforming of methane over Co-Mo/Al<sub>2</sub>O<sub>3</sub> catalyst under low microwave power irradiation. *Catal. Sci. Technol.*, 2018, 8, 5315-5324.
- 11 W. Li, X. Jie, C. Wang, J.R. Dilworth, C. Xu, T. Xiao, and P.P. Edwards, MnO<sub>x</sub>-Promoted, Coking-Resistant Nickel-Based Catalysts for Microwave-Initiated CO<sub>2</sub> Utilization. *Ind. Eng. Chem. Res.*, 2020, 59, 6914-6923.
- 12 T. Odedairo, J. Ma, J. Chen, S. Wang, Z. Zhu, Influences of doping Cr/Fe/Ta on the performance of Ni/CeO<sub>2</sub> catalyst under microwave irradiation in dry reforming of CH<sub>4</sub>, *J. Solid State Chem.*, 2016, 233, 166-177.
- 13 F. Zhang, Z. Song, J. Zhu, L. Liu, J. Sun, X. Zhao, Y. Mao, W. Wang, Process of CH<sub>4</sub>-CO<sub>2</sub> reforming over Fe/SiC catalyst under microwave irradiation, *Sci. Total Environ.*, 2018, 639, 1148-1155.
- 14 I. de Dios García, A. Stankiewicz, H. Nigar, Syngas production via microwave-assisted dry reforming of methane, *Catal.Today*, 2021, 362, 72-80.
- 15 R. Li, W. Xu, J. Deng, J. Zhou, Coke-Resistant Ni-Co/ZrO<sub>2</sub>-CaO-Based Microwave Catalyst for Highly Effective Dry Reforming of Methane by Microwave Catalysis, *Industrial & Engineering Chemistry Research*, 2021, 48, 17458-17468.
- 16 F. Zhang, X. Zhang, Z. Song, X. Li, X. Zhao, J. Sun, Y. Mao, X. Wang, W. Wang, Promotion of microwave discharge over carbon catalysts for CO<sub>2</sub> reforming of CH<sub>4</sub> to syngas, *Fuel*, 2023, 331, 125914.

- 17 T. Odedairo, J. Ma, J. Chen, and Z. Zhu, Cr-Doped La-Ni-O Catalysts Derived from Perovskite Precursors for CH<sub>4</sub>-CO<sub>2</sub> Reforming under Microwave Irradiation. *Chem. Eng. Technol.*, 2016, 39, 1551-1560.
- 18 C.M. Marin, E.J. Popczun, T. Nguyen-Phan, D.N. Tafen, D. Alfonso, I. Waluyo, A. Hunt, D.R. Kauffman, Designing perovskite catalysts for controlled active-site exsolution in the microwave dry reforming of methane, *Appl. Catal. B-Environ.*, 2021, 284, 119711.